Effect of Elongated Graphite on Mechanical Properties of Hot-Rolled Ductile Iron

J. Shi, S. Zou, R.W. Smith, and J.J.M. Too

The mechanical properties of hot-rolled and then annealed ductile iron were evaluated. The deformation of this two-phase material and the effects of the elongated graphite spheres on the mechanical properties and the development of anisotropy of mechanical properties were studied. An attempt was made to describe the anisotropy of tensile strength in terms of the deformation of graphite spheres and of the root curvature, area fraction, and the interbridges that result in disproportional changes of stress concentration, loading capacity, and the tendency to break the interbridges and link the neighboring deformed graphite spheres.

Keywords
ductile iron, mechanical properties, graphite aspect ratio

1. Introduction

THE plastic working of a ductile iron recently became an item of considerable interest to both researchers and the industry. Numerous papers have been published on the workability, deformation, related microstructures, and the mechanical properties of ductile iron (Ref 1-10). The mechanical anisotropy of rolled ductile iron also was evaluated by Sheffler and Libsch (Ref 11).

Deformation, especially the hot deformation of ductile iron, attracts attention because: (a) it refines the as-cast structures, closes up the internal shrinkage cavities and gas porosity, and reduces the segregations of alloying elements; (b) it increases the dimensional accuracy and surface finish of the products; and (c) it reduces energy consumption and manufacturing cost.

Also, because of excellent wear resistance, high damping capacity, and better corrosion resistance, forged ductile iron products have been promoted as replacements of some types of steel forgings. However, before pressing ductile iron to commercial applications, evaluate the mechanical properties and the mechanical anisotropy of potential products.

Extensive work on the effect of inclusions on the mechanical properties and fracture behavior of steels has been reported by many investigators (Ref 12-15). Ductile sphere iron is essentially a steel matrix with graphite inclusions. Obviously, inclusions and second-phase particles can play an important role in determining the mechanical properties and workability of materials because cracks tend to be initiated at such particle/matrix interfaces. Usually, the mechanical behavior depends on the type, shape, volume-fraction, and distribution of the inclusions or second-phase particles. For plastically deformable inclusions, such as spherical graphite in ductile iron, during plastic deformation such as rolling, the inclusions deform with the matrix and become elongated and cause the material to display anisotropic mechanical properties.

J. Shi, S. Zou, and **R.W. Smith,** Materials & Metallurgical Engineering Department, Queen's University, Kingston, Ontario, Canada K7L 3N6; and **J.J.M. Too,** PMRL/CANMET, Department of Energy, Mines and Resources, Ottawa, Canada, K1A 0G1

In this study, the deformation of the spheroidal graphite and its relationship to the gross body deformation was investigated together with an analysis of the effect of the presence of elongated spherical graphite on the mechanical anisotropy.

2. Experimental

The ductile iron was supplied by QIT-Fer-el-Titane, Inc.; its composition is listed in Table 1.

The one-inch thick plates of ductile iron were heated to 1000 °C, soaked for 1 h, then hot-rolled to 20, 35, 50, and 75% reductions. Several passes were used to obtain these reductions, and the specimens were reheated after the rolling operation.

Both the rolled and unrolled materials were then annealed to obtain a ferritic structure. For comparison, a cast steel with a similar composition to that of the matrix material was also hot rolled and annealed.

All materials were then machined to provide specimens parallel and transverse to the rolling directions (Fig. 1). The specimens for measuring the elastic moduli were machined as 120.3 mm × 14.2 mm × 3.85 mm plates, and the plate tensile specimens were produced as standard ASTM B557 subsize 3.85-mm-thick specimens. The tensile test was carried out on an Instron machine. The elastic moduli of the specimens were measured using an acoustic vibration method (Ref 16).

Unnotched impact specimens of 10 mm × 10 mm × 55 mm were machined longitudinally and transversely from the rolled

Table 1 Composition of ductile iron

Element	Composition, wt.%
C	3.32
Si	2.35
Ni	2.11
S	0.01
Mn	0.01
Mo	0.004
Cu	0.6
P	0.022
Cr	0.046
V	0.04
Co	0.033
Ti	0.031

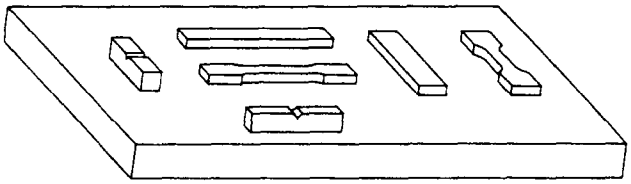

Fig. 1 Position from which the testing specimens were taken from the rolled ductile iron plate

plates for the impact test. During the impact test, the rolled surface of all the specimens faced the impact loading direction.

The deformation of the graphite regions was measured using a Vidas image analyzer.

3. Results and Discussion

Ductile iron is a two-phase mixture of steel (matrix) and graphite spheres. The matrix can be ferritic, pearlitic, or ferritic-pearlitic. For simplicity, a ferritic matrix was chosen for this study; it was obtained by an annealing procedure. This provides an ideal material for the study of the effect of soft inclusions on the mechanical properties of a duplex material. During plastic deformation, the spherical graphite will deform with the matrix; this deformation can be measured. As noted earlier, the ductile iron was first hot rolled to various reductions; i.e., 20, 35, 50, and 75%. In order to remove the effects of work hardening and texture produced during the deformation, both the undeformed and deformed specimens were annealed to get a ferritic matrix. During annealing, the deformed graphite will not change except for a little dissolving into the matrix during heating and depositing on the surface of the deformed graphite spheres during cooling. This was considered to be of little consequence in determining the graphite deformation.

3.1 *Plastic Deformation of Ductile Iron During Hot Rolling*

The plastic deformation of ductile iron during homogeneous compression was reported (Ref 17). The relationship between graphite deformation, matrix deformation, and gross reduction can be expressed as follows:

$$K = \frac{R_i}{R_m} \qquad \text{(Eq 1)}$$

$$K = \frac{F(1 - P^{2/3})}{R_t(1 + F) - (1 - P^{2/3})} \qquad \text{(Eq 2)}$$

where K is deformation ratio of graphite to matrix, F is the ratio of average original matrix height to average original graphite height, P is aspect ratio of the graphite, R_i is graphite reduction, R_m is matrix deformation, and R_t is the total redu ction.

This relationship is used to describe the plastic deformation of ductile iron during hot rolling. In this, the graphite spheres become elongated. Because the width of the plate is much larger than its height before rolling, the deformation during rolling is considered to be plane strain deformation, i.e., the originally spherical graphite will be elongated without change in width. Then the deformation of graphite nodules is determined by the aspect ratio of the deformed graphite spheres. For simplicity, suppose the elongated graphite is a rectangular volume. Its deformation may be expressed in terms of a reduction R along the axis of thickness by the general equation:

$$R = \frac{h_o - h_f}{h_o} \qquad \text{(Eq 3)}$$

where h_o and h_f are the original and final heights (or thicknesses) of the deforming piece. Further assume the volume of a graphite region remains constant; then

$$1/6 \times \pi \times D^3 = h \times D \times l \qquad \text{(Eq 4)}$$

where D is diameter of the sphere and the width of the deformed sphere. Here the width of the sphere is not changed because it is assumed to be a plane strain deformation. h is the height of the deformed graphite sphere, and l is the length of the deformed graphite sphere.

The corresponding reduction of the sphere will be:

$$R = \frac{D - h}{D} \qquad \text{(Eq 5)}$$

From Eq 2:

$$D = \sqrt{\frac{6\,h\,l}{\pi}}$$

Substitute in Eq 2 and 3 and simplify:

$$R = 1 - \sqrt{\frac{\pi\,h}{6\,l}} \qquad \text{(Eq 6)}$$

Assume that the aspect ratio of the elongated sphere is:

$$p = \frac{h}{l} \qquad \text{(Eq 7)}$$

Then substitute this into Eq 4. The reduction of a spherical graphite inclusion in terms of its aspect ratio will be:

$$R_i = 1 - \sqrt{\frac{\pi\,p}{6}} \qquad \text{(Eq 8)}$$

The ratio of the gross reduction to the reduction of the inclusion is:

Table 2 Inclusion-matrix deformation ratio

Specimen	R_t, %	P	K
1	21	0.49 ± 0.01	3.26
2	36	0.29 ± 0.01	1.96
3	55.7	0.14 ± 0.01	1.39
4	75.4	0.057 ± 0.004	1.13

$$\frac{R_t}{R_i} = \frac{\dfrac{h_o - h_f}{h_o}}{(1 - \sqrt{\dfrac{\pi p}{6}})} \qquad \text{(Eq 9)}$$

Combine Eq 7 with 2 to yield:

$$\frac{\dfrac{h_o - h_f}{h_o}}{(1 - \sqrt{\dfrac{\pi p}{6}})} = \frac{1}{1+F} + \frac{F}{K(1+F)} \qquad \text{(Eq 10)}$$

After simplifying Eq 10, the ratio of the inclusion deformation to the matrix deformation can be obtained in the following form:

$$K = \frac{F\,(1 - \sqrt{\dfrac{\pi p}{6}})}{R_t(1+F) - 1 + \sqrt{\dfrac{\pi p}{6}}} \qquad \text{(Eq 11)}$$

Equations 10 and 11 show that if the initial and final height of the specimen (the gross reduction), the final average aspect ratio of the inclusions after rolling, and the original average ratio of matrix height to inclusion height before rolling are known, the ratio of inclusion to the matrix deformation can be obtained.

The original matrix height and inclusion height elements were measured in an undeformed specimen using the image analyzer. Then the average original matrix height, h_{mo}, and inclusion height, h_{io}, were calculated from these elements, and the ratio F ($=h_{mo}/h_{io}$) was found to be 5.08 ± 0.32. The aspect ratios of the rolled specimens were also measured with the image analyzer. After F, p, and R_t were known, the inclusion-matrix deformation ratio, K, could be calculated from Eq 11; the results are listed in Table 2.

The relationship between the inclusion-matrix deformation ratio and the gross reduction is shown in Fig. 2. As the reduction percentage increases, the inclusion-matrix deformation ratio, K, decreases to 1.

3.2 *Mechanical Properties*

Most metals display mechanical anisotropy after plastic deformation. In general, the mechanical properties are always better in the rolling direction than in the transverse direction. This is due to the alignment of deformed inclusions in the rolling direction and/or the formation of the texture. The anisotropy of properties will result in directional workability and fracture behavior. Therefore it is advantageous to be able to predict the anisotropy of mechanical properties caused by the deformed inclusions, especially for hot-rolled ductile iron. The results of the experiments performed here, namely the variations of tensile strength, elastic modulus, elongation, and impact strength with rolling reduction are shown in Fig. 3 through 6.

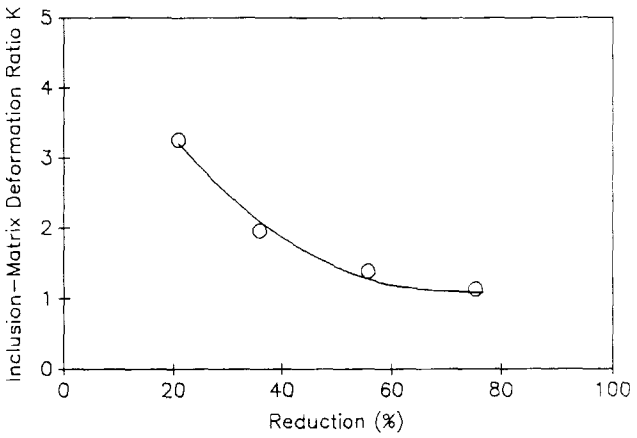

Fig. 2 Relationship between the ratios of inclusion deformation to matrix deformation and the gross reduction

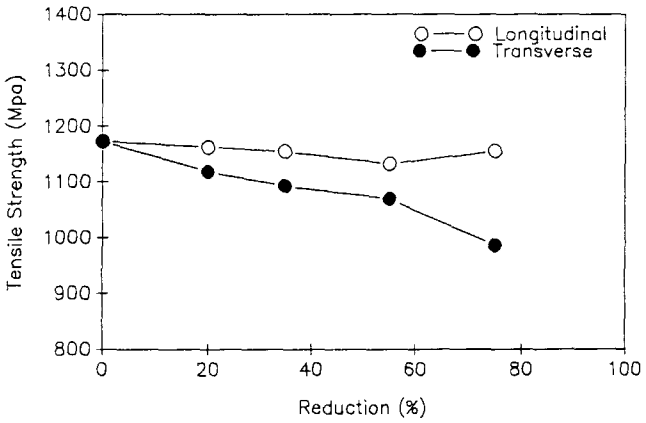

Fig. 3 Tensile strength/reduction curves for rolled ductile iron

3.3 *Tensile Strength*

Figure 3 is the plot of the tensile strength versus the gross reduction for the hot-rolled and then annealed ductile iron. Whereas the tensile strength changes little in the longitudinal direction, a marked decrease, to 17%, occurs in the transverse direction as the reduction increases to 75%. Similar results have been reported by other researchers, but no reason was given (Ref 18). However, we attribute this to: (a) the stress concentrations at the root of the deformed graphite, (b) the loading areas of the matrix, and (c) the interbridges between the elongated graphite spheres.

A rolled graphite sphere is projected onto the x, y, and z planes of the coordinate system as shown in Fig. 7. The difference in radius of the roots of a deformed graphite sphere in the x, y, and z directions can be clearly seen. Here the root is de-

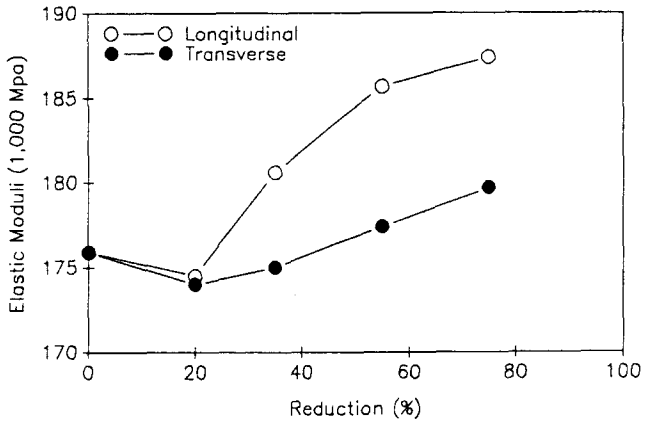

Fig. 4 Elastic modulus/reduction curves for rolled ductile irons

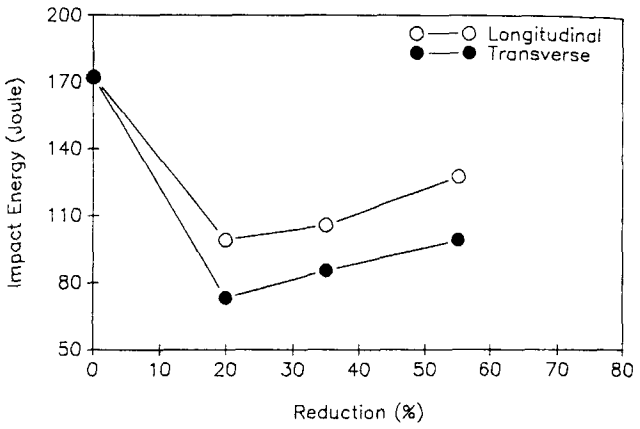

Fig. 6 Impact energy/reduction curves for rolled ductile iron

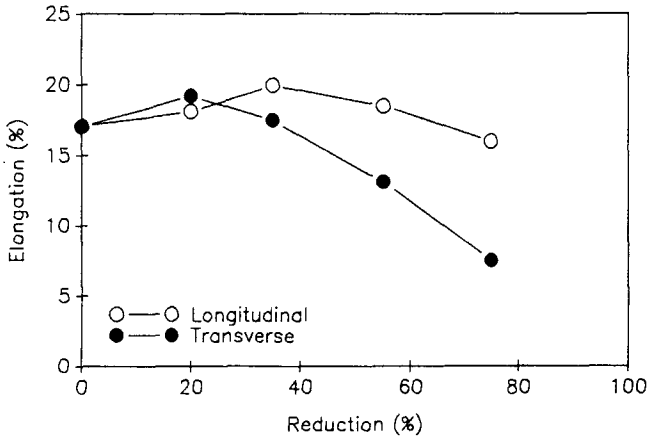

Fig. 5 Elongation/reduction curves for rolled ductile iron

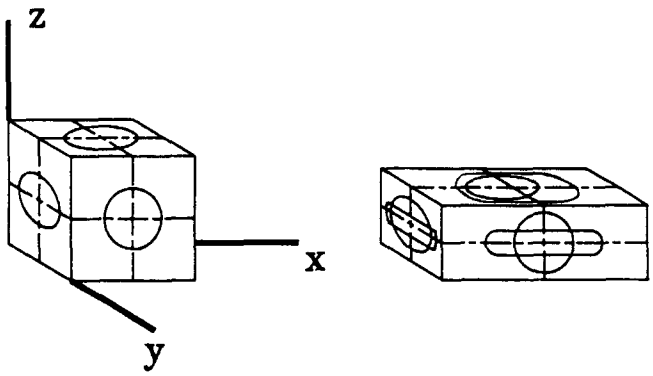

Fig. 7 Schematic showing projections of a rolled graphite sphere upon the orthogonal planes

fined as the two ends that are perpendicular to the reference direction of a cross section in any coordinate plane. The radius ρ_x in both the *x*-*y* and *x*-*z* planes becomes infinite because the graphite sphere is elongated in the rolling direction and the matrix-graphite interface is almost parallel to the rolling direction (*x*). The radius ρ_y in the *x*-*y* plane remains the same as ρ_o, the original root radius of the graphite sphere before deformation, because the earlier rolling produced plane strain deformation. The radius ρ_z in the *z*-*x* and *z*-*y* planes becomes smaller; i.e., the roots become sharper, as the rolling reduction is increased.

Normally the stress concentration factor k_σ can be determined from the radius ρ and the width b of the cross section (Ref 19), namely:

$$k_\sigma = 1 + \sqrt{\frac{2b}{\rho}}$$

The stress concentration factors of a deformed graphite sphere in *x*, *y*, and *z* directions are:

$$k_{\sigma x} = 1 + \sqrt{\frac{2b}{\rho_x}} = 1 + \sqrt{\frac{2b}{\infty}} = 1$$

$$k_{\sigma y} = 1 + \sqrt{\frac{2b}{\rho_y}} = 1 + \sqrt{\frac{2b}{b/2}} = 3$$

$$k_{\sigma z} = 1 + \sqrt{\frac{2b}{\rho_z}} = \sqrt{\frac{2b}{\rho_z}}$$

when $b > \rho$.

Obviously $k_{\sigma z} > k_{\sigma y} > k_{\sigma x}$; therefore, the tensile strengths of the hot-rolled ductile iron in the *x*, *y*, and *z* directions will be:

$$S_x > S_y > S_z$$

resulting in anisotropy of tensile strengths.

Two important factors in determining the anisotropy of tensile strength are the loading area and area of interbridges; i.e., the matrix area between neighboring graphite regions.

The loading area here refers to the cross-sectional area of the matrix, not the total cross-section. Because the deformed graphite spheres are usually supposed to have no strength, their cross sections cannot be included in the real loading area. Therefore, any change of area fraction of the deformed spherical graphite in the total cross section will result in a correspond-

Table 3 Loading area

Area of graphite	Area fraction of graphite	Loading area	Strength
$A_x = h_i D = (1/k)\, hD = hD/k$	↓	↑	↑
$A_y = h_i l_i = (1/k)\, hkl = hl$	1	...	...
$A_z = Dl_i = Dkl = kDl$	↑	↓	↓

Table 4 Interbridge

Interbridge	Tendency to break	Loading direction
$Ib_x = (1/k) Ib_{xo}$	↑	y or z
$Ib_y = Ib_{yo}$	...	x or z
$Ib_z = k \times Ib_{zo}$	↓	x or y

ing change of loading capacity; i.e., the tensile strength. The predicted results are shown in Table 3. Clearly,

$$S_x > S_y > S_z$$

due to the change of loading area in the x, y, and z directions.

As discussed earlier, the reduction of height of a deformed graphite sphere is:

$$R_i = K R_m$$

where $K > 1$. In order to keep the volume of the deformed graphite sphere constant, the elongation, i.e., the increase of the length of the deformed graphite sphere, should be larger than that of the matrix because the width of a deformed graphite sphere will not change if the specimen is subjected to only plane strain deformation. This will result in a disproportionate change of loading area and interbridges between the neighboring graphite regions in the x, y, and z directions.

The change in the loading areas and the interbridges may be summarized in Tables 3 and 4 where A_x, A_y, and A_z are the cross-sectional areas of a deformed graphite sphere in the x, y, and z directions; h_i and l_i are the final height and length of a graphite sphere after deformation; h and l are the final height and length of a matrix element of an original shape equivalent to that of the graphite sphere; D is the diameter of a graphite sphere; Ib_x, Ib_y, and Ib_z are the interbridges in the x, y, and z directions; and Ib_{xo}, Ib_{yo}, and Ib_{zo} are the interbridges in the x, y, and z directions when the graphite spheres are replaced by the matrix material after deforming in the same reduction.

Table 4 shows that there are two different interbridges affecting the tensile strength in each direction. For example, Ib_x increases the tendency to break the interbridges and link up the neighboring deformed graphite spheres, and conversely, Ib_z decreases the tendency to break the interbridges and link up the neighboring deformed graphite spheres when it is loaded in the y direction. This tendency appears to be balanced by the two opposite signs, but it is not. Because a crack always initiates and propagates from the weakest site of the material, the tensile strength here should be determined by the worst condition; i.e., the interbridge Ib_x to increase the tendency to link up the neighboring deformed graphite spheres for loading in the y direction.

Therefore, for loading in the x direction, there is no tendency to break the interbridge Ib_y and link up the neighboring deformed graphite spheres. For loading in the y direction, the tendency to break the interbridge and link up the neighboring deformed graphite spheres will increase. Loading in the z direction will increase the tendency to break the interbridge and link the neighboring deformed graphite spheres as well, but the increasing tendency to break and link up will be more severe when loading in the z direction than in the y direction because of the effect of the second interbridge for each of these directions. This results in an anisotropy of fracture tendency; i.e., the anisotropy of tensile strength in the x, y, and z directions:

$$S_x > S_y > S_z$$

Geometrically, there are three factors affecting the anisotropy of tensile strength of a hot-rolled and annealed ductile iron: root radius (root sharpness), loading area, and interbridge. Each of them causes some variation of stress concentration, loading capacity, and tendency for the linking up of the neighboring deformed graphite spheres. These factors result in:

$$S_x > S_y > S_z$$

However, the stress concentration factor is the most effective and, hence, most important factor in its effect on the anisotropy of tensile strength among the three; i.e., the difference of tensile strength caused by stress concentrations in the x, y, and z directions are very large.

In this study, experimentally determined values of the tensile strength in the rolling direction (x direction) do not change much with percentage reduction. This is because the sizes of the interbridges in the z direction (the through-thickness direction) become smaller. Thus they are easier to break although the thinning rate of the matrix is much smaller than that of the deformed graphite spheres. This reduces the strength and balances the increase in strength due to the reduction of the stress concentration at the roots of the deformed graphite regions in this direction.

In the transverse direction (y direction), the tensile strength decreased to 17% as the rolling reduction increased to 75%. The main reason for this is that the change of interbridge distance Ib_x, as listed in Table 4, increases the tendency to break the interbridge and to link up the neighboring deformed graphite regions. Thus the tensile strength is reduced, although the stress concentrations at the root of the deformed graphite regions in the transverse direction do not increase, as shown in Fig. 7.

The tensile strength in the "through-thickness" z direction was not measured in this study because it is less practical to use, and it is not possible to make adequate tensile specimens for this direction. However, the tensile strength of the rolled ductile iron in this direction could be the lowest among all three directions because the stress concentration at the roots of the deformed graphite spheres is the highest in this direction, as compared to the other two directions. In addition, the loading area in the z direction is the smallest; the interbridges between the deformed spheres are also the smallest. When the rolling reduction increases, a lamellar structure is developed, thus reduc-

ing the loading area and, hence, making the material easier to tear.

However, the ease of crack initiation and propagation in the rolled material differs with the direction considered. The main factors affecting this are: (a) the stress concentration at the root of the deformed inclusions or pores, which depends on the sharpness of the roots of the deformed inclusions or pores; (b) the loading area of the matrix; and (c) the interbridges between the deformed graphite regions.

3.4 *Elastic Modulus*

As expected, the elastic modulus of a fiber-reinforced composite is always higher in the direction of the fiber alignment and lower in the transverse and through-thickness directions. Interestingly, similar results were obtained in this study for the hot-rolled and then annealed ductile iron. Here the intrinsic frequency (Ref 16) of the specimens was measured by an acoustic vibration test; then the elastic moduli were calculated from the resonant frequency, f, by the following modified equation:

$$E = \psi \frac{l^4 \rho}{t^2} f^2$$

where E is the elastic modulus (Pa), ψ is the coefficient (here first mode is 9.66×10^{-4}), l is the length of the bar (m), ρ is the density of the material of the bar (kg/m^3), t is the thickness of the bar (m), and f is the frequency (Hz).

The modulus versus rolling reduction data were plotted in Fig. 4. Both moduli (in the longitudinal and transverse directions) increase as the rolling reduction increases, but the rate of increase is much higher in the longitudinal direction than in the transverse direction. Because the specimens were machined from the hot-rolled plate, then annealed, and finally surface ground, there is not much work hardening present. Thus the observed effects cannot be due to work hardening. They may be the results of the elongated graphite or the rolling texture. In order to investigate the effects of rolling texture on the elastic moduli of hot-rolled and then annealed ductile iron, the elastic moduli of hot-rolled then annealed cast ferritic steel were also measured and calculated. No clear relationship between the elastic modulus and the rolling reduction was observed in the rolled cast ferritic steel. Therefore, the increase of elastic modulus with the increasing rolling reduction is probably attributable to the presence of the elongated graphite. The spherical graphite is brittle and so becomes highly fractured after the cold rolling of the ductile iron. This could be easily revealed by deep etching. However, the effects of hot rolling differ quite considerably from cold rolling. In fact, hot rolling represents both hot pressing and sintering. The spherical graphite in the matrix was effectively hot pressed during hot rolling and sintered during annealing. Thus, surprisingly, it behaved as fiber-aligned metal matrix composite, showing an increased elastic modulus in both the longitudinal and transverse directions.

3.5 *Elongation*

The effect of hot rolling on elongation is shown in Fig. 5. In both the longitudinal and transverse directions, the elongation decreases with increase in percentage reduction, the rate of decrease being greatest in the transverse direction.

3.6 *Impact Strength*

One of the most important mechanical properties of ductile iron in service is the toughness, which is usually measured by some impact test. Figure 6 shows that the impact strengths first drop sharply at 20% rolling reduction. Then, as the rolling reduction increases, it increases gradually in both the longitudinal and transverse directions. In the meantime, the anisotropy of impact strength develops. The impact strength in the transverse direction is almost ~75% of that in the longitudinal direction for all the reductions above 20%. This increase in the impact strength is inversely proportional to that of the decrease of the elongation with percentage reduction.

4. Conclusion

- For hot-rolled and then annealed ductile iron, the tensile strength does not change much in the longitudinal direction but decreases in the transverse direction. The elastic modulus and impact strength increase in both longitudinal and transverse directions as the rolling reduction increases. The elongation in both longitudinal and transverse directions decreases as the rolling reduction increases, but the rate of decrease is higher in the transverse direction than in the longitudinal direction.
- The development of anisotropy of mechanical properties may be attributed to the presence of the elongated graphite spheres and the tendency to break the interbridges and link the neighboring deformed graphite spheres.
- It is possible to make high-strength machine components from ductile iron by hot deformation followed by austempering (Ref 20).

Acknowledgments

This work was supported in part by DSS contract No. 20ST 23440-4-9327, Department of Energy, Mines and Resources (EMR), Government of Canada and by the National Science and Engineering Research Council of Canada.

This project forms part of the near-net shape processing program of Professor R.W. Smith.

References

1. J.A. Perry and J.E. Rehder, *Iron Age*, Vol 168 (No. 14), 1951, p 229-233
2. Wakamoto, J. Saga, and T. Tanaka, *Rep. Osaka Munic. Inst. Ind. Res.*, Vol 4 (No. 2), 1952, p 18-21 (in Japanese)
3. E.P. Unksow and D.I. Berezhkovskii, *Vestn. Mashinostr.*, Vol 33 (No. 12), 1953, p 29-35
4. K. Okabayashi, *Imono (J. Jpn Foundrmen's Soc.)*, Vol 40 (No. 3), 1969, p 233-235
5. S. Riegger, O. Vöhringer, and E. Macherauch, *Giessereiforschung*, Vol 23 (No. 1), 1971, p 32-38 (in English)
6. L.A. Neumeier, B.A. Betts, and R.L. Crosby, *Trans. AFS*, Vol 84, 1976, p 437-448
7. Forging Industry Education and Res. Foundation, Cleveland, Ohio, "Evaluation of Die Forging of Ductile Iron," U.S. Depart-

ment of Commerce, National Technical Information Service PB-271 791, June 20, 1977

8. N.M. Jha and M. Ram, *Indian J. Technol.*, Vol 19 (No. 2), Feb 1981, p 55-63
9. X.J. Zhang and G.H.J. Bennett, *Ironmaking Steelmaking*, Vol 15 (No. 6), 1988, p 323-328
10. K.P. Zamula, A.M. Petrichenko, and L.A. Solntsev, *Steel USSR*, Oct 1977, p 595-597
11. K.D. Sheffler and J.F. Libsch, *Transactions of the ASM*, Vol 61, 1968, p 203-209
12. A.J. DeArdo, Jr. and E.G. Hamburg, *Sulfide Inclusions in Steel*, proceedings of an international symposium, 1974, American Society for Metals
13. L.G. Séraphin and R.H. Tricot, *Sulfide Inclusions in Steel*, proceedings of an international symposium, 1974, American Society for Metals
14. W.J. McG. Tegart and A. Gittins, *Sulfide Inclusions in Steel*, proceedings of an international symposium, 1974, American Society for Metals
15. J. Kozasu and J. Tanaka, *Sulfide Inclusions in Steel*, proceedings of an international symposium, 1974, American Society for Metals
16. B. Rayleigh, *The Theory of Sound*, Dover Publications, 1945
17. J. Shi, "Deformation Models and The Workability Criterion of The Soft Inclusion-Containing Materials Based on Local Strain Measurements," Ph.D. thesis, Materials and Metallurgical Engineering Department, Queen's University, Canada, 1992
18. L.A. Neumeier, B.A. Betts, and R.L. Crosby, *Trans. AFS*, Vol 84, 1976, p 437-448
19. A.S. Teleman and A.J. McEvily, Jr., *Fracture of Structural Materials*, John Wiley & Sons, 1967
20. J. Shi, S. Zou, J.J.M. Too, and R.W. Smith, "On The Quenchability of Austempered Ductile Iron," *Cast Met.*, Vol 3 (No. 2), 1992